**Structural Engineering and Mechanics**, *Vol. 56, No. 1 (2015) 1-25*
DOI: http://dx.doi.org/10.12989/sem.2015.56.1.001 

# Prefabricated-HSPRCC panels for retrofitting of existing RC members-a pioneering study

Idris Bedirhanoglu*

*Department of Civil Engineering, Dicle University, 21280, Diyarbakir, Turkey*

*(Received September 20, 2014, Revised February 9, 2015, Accepted May 20, 2015)*

**Abstract.** The main goal of this study was to develop a convenient strengthening technique for retrofitting of reinforced concrete members. For this purpose a new retrofitting material so-called prefabricated-HSPRCC (high performance steel plate reinforced cementitious composite) panel was developed by using high performance concrete and perforated steel plate. Prefabricated-HSPRCC composes advantages of steel and high performance concrete. The prefabricated-HSPRCC panels were either only bonded on the specimens using epoxy mortar or anchored to the specimen by steel bolts as well as bonding. Effect of different variations such as prefabricated-HSPRCC panel thicknesses, steel plate thicknesses, puncture orientation of perforated steel plate, existence of anchorage etc. were studied through a simple experimental work. The behaviour of the specimens under vertical point load was also studied by using simple mechanics. The retrofitted specimens were found to exhibit much better performance both in terms of strength and deformation capability. The anchorage application was found to positively affect this improved performance. Furthermore, as a result of the tests the best parameters of prefabricated-HSPRCC plate for improving strength and deformation capacities were determined.

**Keywords:** cement; concrete panel; confinement; ductility; steel plate reinforced cementitious composite; HSPRCC; retrofitting; shear

## 1. Introduction

Many reinforced concrete structures do not meet the requirements given by current building design codes by various aspects. Lack of adequate shear strength of beam-column joints and captive columns is among the most common deficiencies. Research conducted on the shear behaviour of the beam-column joints strengthened with innovative materials is rare, (Gergely *et al*. 2000, Ghobarah and Said 2001, Amoury and Ghobarah 2002, Prota *et al*. 2003, Antonopoulos and Triantafillou 2003, Mukherje and Joshi 2005, Pantelides *et al*. 2008, Ilki *et al*. 2008, Hamad and Ibrahim 2009, Yen *et al*. 2010). Research on the shear behaviour of retrofitted concrete panels is also limited (Yoshitake *et al*. 2006, Ilki *et al*. 2007, Bedirhanoglu *et al*. 2008). Bedirhanoglu (2009) mentioned various recent retrofitting materials in his literature survey on joint including retrofitting of captive columns and panels. After widely used steel (Biddah *et al*. 1997, Nagaprasad *et al*. 2009, Lin *et al*. 2010, Yen and Chien 2010) and reinforced concrete jacketing (Alcocer and

*Corresponding author, Assistant Professor, E-mail: idrisbed@gmail.com


http://www.techno-press.org/?journal=sem&subpage=8 ISSN: 1225-4568 (Print), 1598-6217 (Online)

Jirsa 1993, Tsonos 2002, Karayannis *et al*. 2008, Tsonos 2010), researches have been concentrated on the user friendly innovative materials such as FRP (fiber reinforced polymers) (Karbhari and Gao 1997, Xiao and Wu 2000, Gergely *et al*. 2000, Mosallam 2000, Amoury and Ghobarah 2002, Prota *et al*. 2003, Antonopoulos and Triantafillou 2003, Xiao 2004, Mukherje and Joshi 2005, Karayannis and Sirkellis 2008, Ilki *et al*. 2008, Durham *et al*. 2009, Pantelides *et al*. 2008, Tsonos 2008, Niroomandi *et al*. 2010, Garcia *et al*. 2010, Barros *et al*. 2011, Ilki *et al*. 2011, Abdulhamed *et al*. 2013) and steel fiber reinforced concrete (Shah 1991, Li *et al*. 1993, Shannag *et al*. 2001, Shannag *et al*. 2005, Lu and Hsu 2006, Ilki *et al*. 2009). Cement based fiber reinforced composite sheets also has been used by Wu *et al*. (2010) as a retrofitting material. Recently Bedirhanoglu *et al*. (2013), Lee *et al*. (2013) work on precast fiber reinforced cementitious composites for seismic retrofit of deficient rc joints.

In the literature, a small number of studies have been conducted on the behaviour of retrofitted reinforced concrete members with low-strength concrete. In addition, to the best of the author's knowledge, no technical report is currently available concerning the seismic retrofitting of RC members with prefabricated-HSPRCC plates.

Like many studies in literature primary purpose of this study is to develop an innovative material could be used for retrofitting reinforced concrete members especially beam-column joints

Table 1 Specimen details

| No | Specimens | Steel plate thicknesses (mm) | HSPRCC thicknesses (mm) | Anchorage | Presence of steel plate * | Hole orientation | Age of the concrete panel and HSPRCC panel at the testing days (day) |
|---|---|---|---|---|---|---|---|
| 1 | DS-O-a | - | - | - | - | - | 140/- |
| 2 | DS-O-b | - | - | - | - | - | 141/- |
| 3 | DS-O-c | - | - | - | - | - | 149/- |
| 4 | DS-HSPRCC-30-1-CD1-A | 1 | 30 | Present | D | CD1 | 362/185 |
| 5 | DS-HSPRCC-30-2-CD1-A | 2 | 30 | Present | D | CD1 | 359/182 |
| 6 | DS-HSPRCC-30-1-CD2-A | 1 | 30 | Present | D | CD2 | 365/188 |
| 7 | DS-HSPRCC-20-0.5-D1-A | 0.5 | 20 | Present | F | D1 | 365/186 |
| 8 | DS-HSPRCC-20-0.5-D2-A | 0.5 | 20 | Present | F | D2 | 367/195 |
| 9 | DS-HSPRCC-20-0.5-D3-A | 0.5 | 20 | Present | F | D3 | 368/195 |
| 10 | DS-HSPRCC-20-1-D2-A | 1 | 20 | Present | F | D2 | 367/215 |
| 11 | DS-HSPRCC-20-2-D2-A | 2 | 20 | Present | F | D2 | 367/196 |
| 12 | DS-HSPRCC-20-1-D2 | 1 | 20 | No | F | D2 | 368/210 |
| 13 | DS-HSPRCC-30-1-D2-A | 1 | 30 | Present | F | D2 | 359/185 |
| 14 | DS-HSPRCC-30-2-D2-A | 2 | 30 | Present | F | D2 | 366/192 |
| 15 | DS-HSPRCC-30-3-D2-A | 3 | 30 | Present | F | D2 | 361/187 |
| 16 | DS-HSPRCC-40-1-D2-A | 1 | 40 | Present | F | D2 | 361/209 |
| 17 | DS-HSPRCC-40-2-D2-A | 2 | 40 | Present | F | D2 | 362/187 |
| 18 | DS-HSPRCC-40-3-D2-A | 3 | 40 | Present | F | D2 | 369/198 |

*D: Diagonal strip, F: Full surface

and captive columns against shear forces. HSPRCC plates with superior properties were developed through a material studies. Performance of this material was tested through a simple panel tests. For this purpose the core of beam-column joints or columns are represented by a concrete panel. A simple representative testing method was utilized for experimental analysis of shear behaviour of low-strength concrete panels retrofitted with prefabricated-HSPRCC panels. Previously, this type of simple testing technique was used by different researchers for similar purposes (Valluzzi *et al*. 2002, Gabor *et al*. 2006, Ilki *et al*. 2007, Bedirhanoglu *et al*. 2008, Bedirhanoglu *et al*. 2013). To carry out the experimental work 18 concrete panel elements were constructed with low-strength concrete, Table 1. Three specimens, which were tested without strengthening, were used as reference specimens. Fifteen specimens were strengthened using prefabricated-HSPRCC plates with different connection details. The specimens were intentionally cast using low-strength concrete for representing majority of relatively old existing reinforced concrete structures, particularly in developing countries. The main parameters in retrofitting technique were thickness of the prefabricated-HSPRCC plate, thickness of the steel plate, holes distribution of the perforated steel plate, presence of the steel plate (full surface or only in diagonal directions) and presence of the mechanical anchorages. More details of the specimens are presented in Table 1.

The test results are evaluated in terms of the strength of the specimen, ductility and deformation performances, as well as failure patterns. According to the obtained results, retrofitting with prefabricated-HSPRCC plates increased the shear strength of concrete panels and changed the very brittle failure mode to less brittle. The behaviour of reference and retrofitted specimens were also evaluated and predicted by using simple mechanic rules. The analysis results and experimental data are in satisfactory agreement in terms of strength.

## 2. Experimental program

### *2.1 Outline of the test method*

A simple test technique was used to evaluate comparative shear strengths of low-strength concrete panels either before or after retrofitting. An Amsler universal testing machine was used to apply the load to the diagonal direction of the specimens. Main target of using this simple test setup was to make a comparative evaluation of the performances of the specimens, rather than obtaining their pure shear behaviour. Starting point of developing this simple test method is back

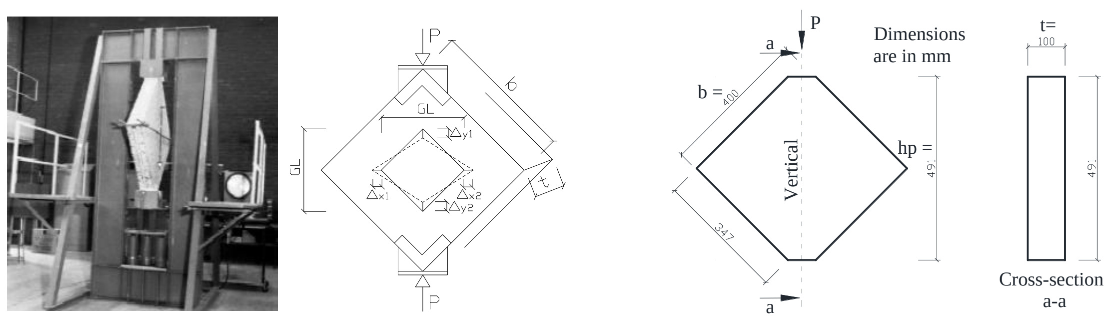


(a) (b)

Fig. 1 (a) Diagonal tension or shear test given by ASTM E 519, (b) detail of test specimens to ASTM E 519 (2002). ASTM E 519 (2002) proposed a test method that covers determination of the diagonal tensile or shear strength of 1.2 by 1.2-m masonry assemblages by loading them in compression along one diagonal (see Fig. 1(a)), thus causing a diagonal tension failure with the specimen splitting apart parallel to the direction of load. Various researchers uses different test setup for shear tests such as Collins *et al*. (1985), Vecchio and Nieto (1991), Kanakubo and Shindo (1997), Itoh *et al*. (2000), Mosallam *et al*. (2003).

To make the testing method simpler and more appropriate for in-plane shear testing instead of steel loading shoes (Fig. 1(a)) two opposite angle of the square specimen were produced truncated (Fig. 1(b)) to make a flat plane for diagonal loading which is the only difference between the test method of ASTM E 519 (2002) and the current test method.

To evaluate the validity of the test method and to choose the best type of loading shoes a series of preliminary (pilot) tests were carried out by Bedirhanoglu (2009). The most convenient ratio (ratio of length of the edge of the loading shoe to the length of the edge of the specimen) for loading shoes of each specimen having different loading tips was determined by using linear finite element analysis (LFEM) while it is suggested to be 1/8 by ASTM E 519 (2002). Among the types of loading tips the one truncated tip was selected considering the simplicity of the testing of that type of specimen and convenient ratio for loading tip was determined as 1/7.5 by Bedirhanoglu (2009).

### *2.2 Details of test specimens*

Experimental study included 18 specimens with 400×400×100 mm dimensions as shown in Fig. 1(b). 15 specimens were retrofitted, while three specimens without retrofit were used as reference specimens. Some details of retrofitting are given in Table 1. For construction of specimens, specially designed ready mixed low-strength concrete with water/cement ratio of 1.17 was used to represent typical low strength-concrete used in existing structures built in Turkey especially before 1990 (Bedirhanoglu *et al*. 2010, Bedirhanoglu 2014). Ordinary Portland cement class 42.5 was used in the mixture. Maximum aggregate size of powdered stone, sand and gravel was 4, 4 and 8 mm, respectively. Concrete mix-proportion is presented in Table 2. The average compressive strength and elasticity modulus of concrete at the day of testing was around 8 and 14000 MPa, respectively. Stress-strain relationship measured 180 days after casting and variation of compressive strength with time are shown in Fig. 2(a) and (b), respectively. Construction of the specimens is shown in Fig. 3(a).

For strengthening, prefabricated-HSPRCC panels were used with different thickness. The prefabricated-HSPRCC panels were either only bonded on the specimen or anchored to the specimen by steel bolts as well bonding. Before bonding the prefabricated-HSPRCC panels on the specimens, surface preparation procedure was carried out, which included sanding and cleaning. Epoxy based adhesive which had the tensile strength of 25 MPa and compressive strength of 75 MPa at the age of 7 days was used for bonding prefabricated-HSPRCC plate to the specimen. The retrofitting steps are shown in Fig. 3b and anchorage application details are shown in Fig. 4(a). As seen in this figure the dimensions of the prefabricated-HSPRCC panels (400×400×$t$ mm, $t$ = 20, 30

Table 2 Concrete mix-proportion (kg/m$^3$)

| Cement | Water | Sand | Gravel | Powdered stone | Superplasticizer |
|---|---|---|---|---|---|
| 180 | 210 | 650 | 880 | 337 | 2.10 |

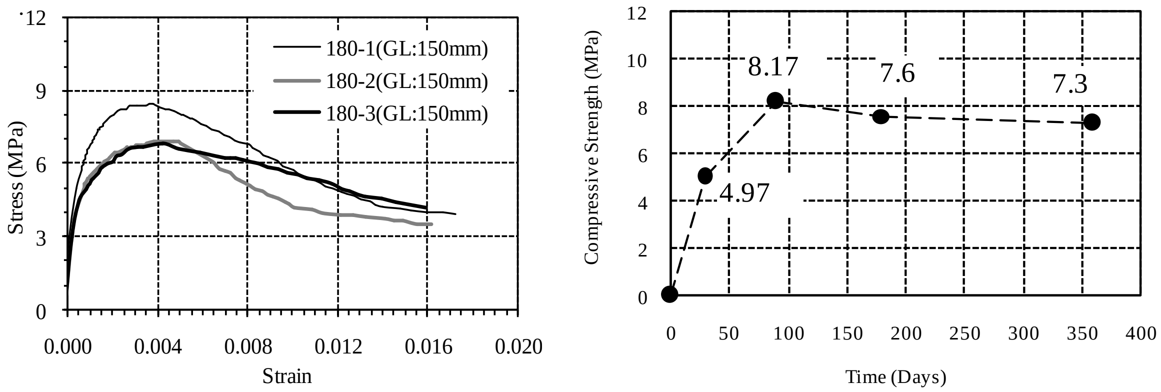


(a) (b)

Fig. 2 (a) Stress-strain relationship, (b) variation of compressive strength with time (each compressive strength is the average of three standard cylinder tests)

(a)

(b)

Fig. 3 (a) Construction of specimens, (b) retrofitting applications of specimens

and 40 mm) were tuned to match the dimensions of the specimens. The thickness of the bonding material between the prefabricated-HSRCC panel and the concrete panel surface was 3 mm. The epoxy adhesive was applied on the prepared surface by a trowel to ensure the uniform thickness of 3 mm of the epoxy adhesive layer. As a further precaution for appropriate connection of prefabricated-HSPRCC panel to the concrete surface all retrofitted specimens except specimen DS-HSPRCC-20-1-D2; four 16-mm diameter rods were used to anchor the prefabricated-HSPRCC panel to the specimen. For fixing the roods, approximately 0.012 kNm torque was applied to the bolts. Tension test was carried out to define mechanical properties of the anchorage rod. According to tension tests yielding stress and elastic modulus were measured to be 577 and 181000 MPa, respectively. Fig. 4(b) shows stress-strain relationship of tension test of steel rod.

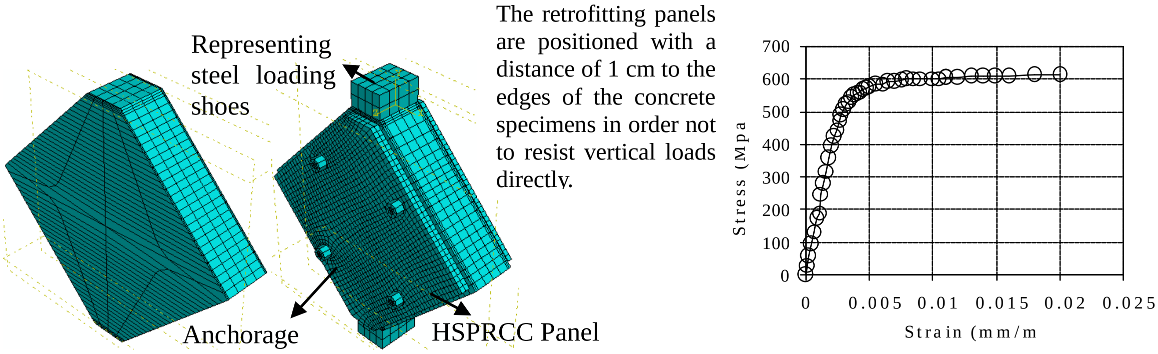


Fig. 4 (a) Anchorage applications, (b) stress-strain relationship of anchorage rod

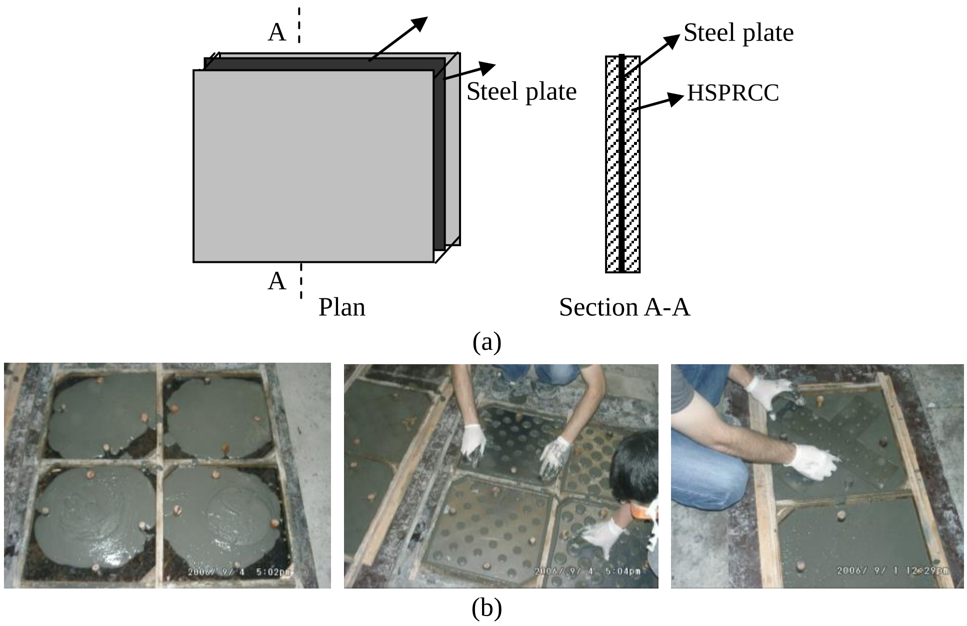


Fig. 5 (a) Composition of HSPRCC plate, (b) prefabrication of HSPRCC panel

### *2.3 Prefabrication of prefabricated-HSPRCC panels*

Prefabricated-HSPRCC panels gathering advantage of steel and cementitious materials by combining of perforated steel plate and high-strength cementitious grout. The main advantage of high performance cementitious mortar is high compression strength capacity while disadvantage is low tensile strength capacity. On the other hand steel plate has the high tensile strength capacity and low compressive strength capacity due to buckling.

Composition of prefabricated-HSPRCC panel is shown in Fig. 5(a). Casting grout for prefabricated-HSPRCC panel is the same as casting concrete. However it should be noted that relatively longer mixing time (≈30 minutes) than would be conducted for normal concrete was necessary to obtain workable prefabricated-HSPRCC mixture. The prefabricated-HSPRCC panels were cast in timber moulds and they were placed on a vibration table to ensure satisfactory consolidation. After placing one layer of high performance grout (which was the half width of the prefabricated-HSPRCC panel) perforated steel plate was placed on the grout and the other one layer of grout was placed to cover steel plate shown in Fig. 5(b).

The panels were removed from the formwork after one day and were cured in 90℃ water for 3 days and in 20℃ water for 25 days. The mix-proportion used in production of prefabricated-HSPRCC panels is given in Table 3. The microsilica was produced by Elkem Materials and had a mean particle size smaller than 500 $\mu$m and a specific gravity of 2.3 kg/dm$^3$. Fig. 6 shows particle size distributions of sands and silica sand which constitute all aggregate of the grout. To obtain mechanical characteristics of the grout, standard cylinder compression and cylinder splitting tensile tests were carried out, Fig. 7. According to material test results of the compressive and tensile strengths of the mixture around testing days were found to be approximately 116 and 8.8 MPa, respectively. Another design problem of prefabricated-HSPRCC panels is perforated steel plates. Steel plates were punctured with different hole orientations. As can be seen in Table 1 presence of steel plate was named as D (Diagonal strip) and F (Full surface) where puncture distribution were named as D1, D2 and D3. Figs. 8-9 show different puncture distributions for full surface and diagonal applications. Material characteristics of steel plates obtained with tension tests. Tension tests were applied for every different plate thickness and in two main directions of each plate. Specimens for tension tests were prepared according to TS138 EN 10002-1 (2004) as can be seen in Fig. 10(a). Fig. 10(b) shows fractured coupons of tension tests and Fig. 11 shows stress-strain relationship of tension tests. As seen in Fig. 16 average yielding stresses are 150 and 300 MPa while maximum stresses are around 300 and 400 MPa for 1 and 3 mm steel plates, respectively.

Table 3 Prefabricated-HSPRCC mix-proportion (kg/m$^3$)

| Cement | Water | Microsilica | Silica sand | Sand | Admixture |
|---|---|---|---|---|---|
| 968 | 212.9 | 193.6 | 580.7 | 290.3 | 34.8 |

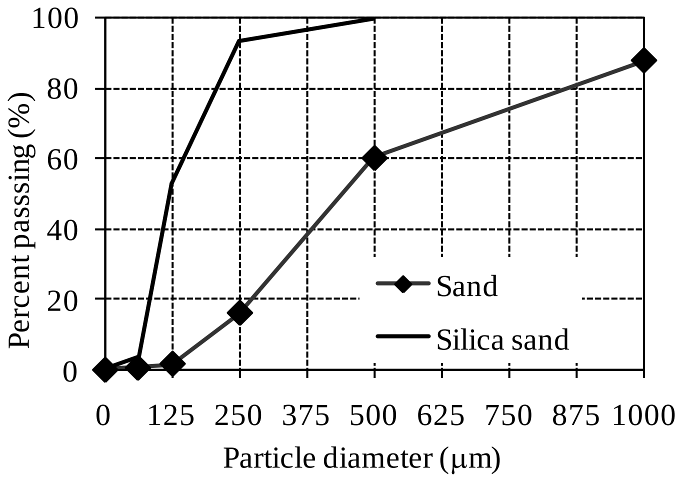


Fig. 6 Particle size distributions of sand and silica sand

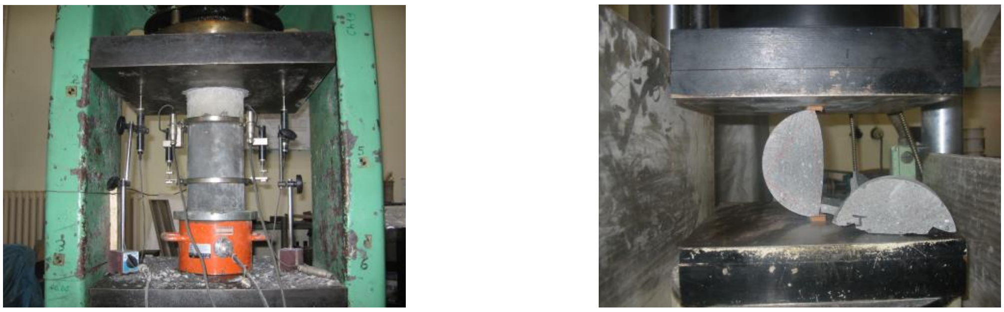

Fig. 7 Material tests

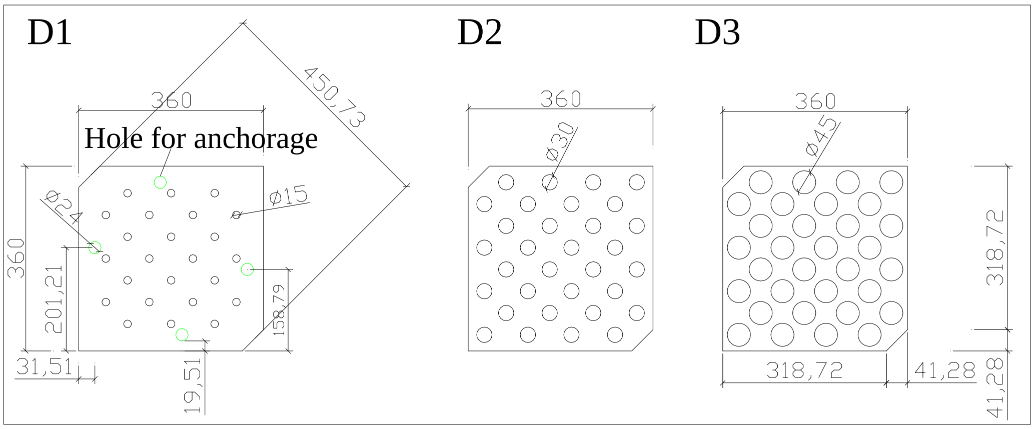


Fig. 8 D1, D2 and D3 puncture configurations of steel plates for full surface application

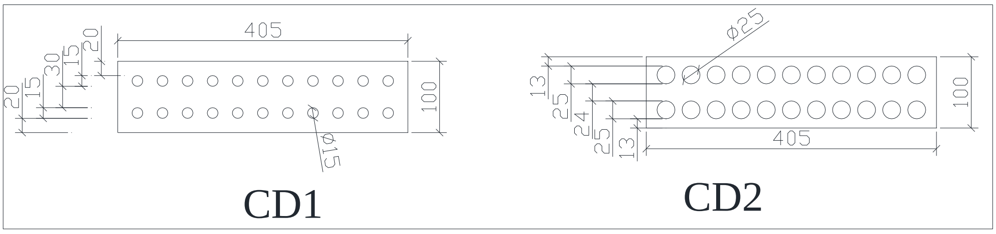


Fig. 9 CD1and CD2 puncture configurations of steel plates for full diagonal application

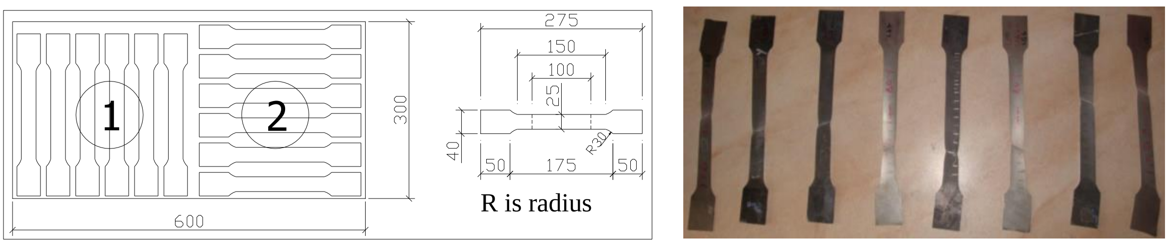


(a) (b)

Fig. 10 (a) Coupons for material tests, (b) tension tests of steel plate coupons

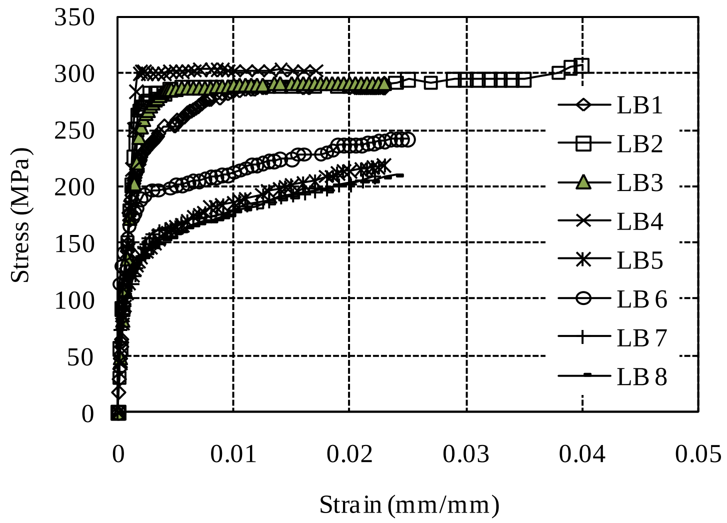


Fig. 11 Stress strain relationship of steel coupon tests (please note that: first four diagrams are for 3 mm and the other is for 1 mm steel plate thickness)


(a) (b)

Fig. 12 Retrofitting with precast panels; (a) application in retrofitting of columns or beams to increase shear force capacity (Ilki *et al* 2009), (b) application in corner or exterior joints (Bedirhanoglu 2009)

### *2.4 Sample applications of the precast plates in the cite*

A brief introduction was provided in this section about the application way of prefabricated plate in the place. Prefabricated plates can be bonded with epoxy to the all faces of the columns or beams. Sample applications are given in Fig. 12 for columns, beams or joints. Further details on the retrofitting with precast panels provided by Bedirhanoglu (2009).

### *2.5 Details of test setup*

Fig. 13 shows the loading setup. An Amsler universal testing machine with the capacity of 5000 kN was used for applying concentric axial compressive loads (vertical loads) on the diagonal of

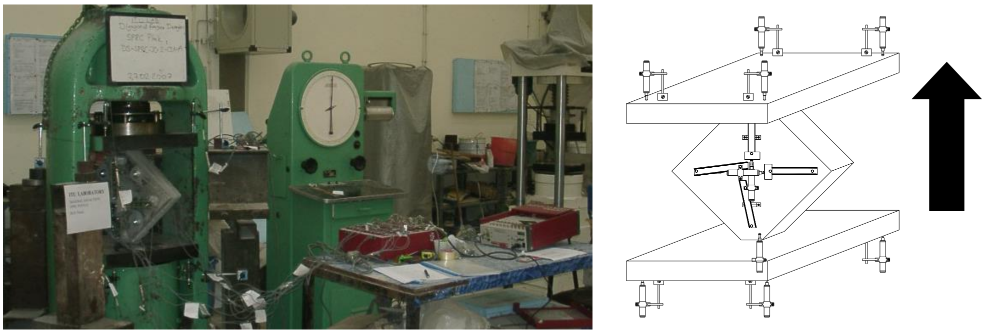

Fig. 13 Test machine and schematic view of loading setup

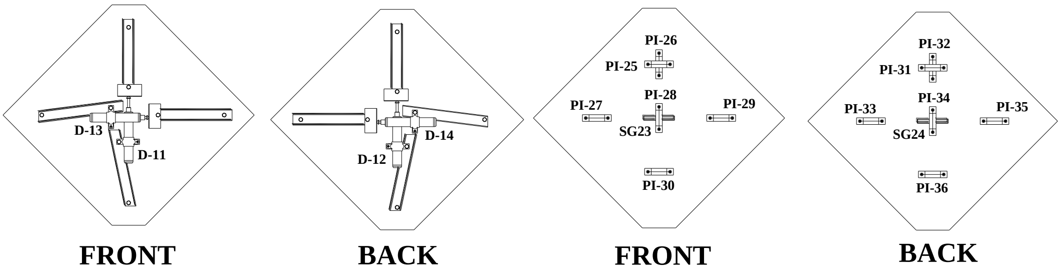


(a) (b)

Fig. 14 Measuring system (a) linear variable displacement transducers (b) pi-type displacement transducers and strain gages

the specimen. Loads applied vertically to the diagonal of the specimens to represent real conditions of reinforced concrete members subjected to shear stress such as joints, columns, shear walls etc. Vertical loads represent diagonal compression loads in shear panel region of such members. Similar test setup and loading system were used before by some other researchers (Valluzzi *et al*. 2002, Bedirhanoglu *et al*. 2013). External vertical displacements at the loading plates were measured with eight linear variable displacement transducers (LVDT). The average deformations of specimens in two principal directions were measured at around 400 mm gage length. For measurement of the displacements and strains at different locations on the specimen, pi-type displacement transducers and strain gages were used in addition to linear variable displacement transducers. Locations of the strain gages, pi-type displacement transducers and linear variable displacement transducers on the specimens are shown in Fig. 14.

## 3. Experimental results

Several results of the experiments are summarized in Table 4. In this table failure modes, shear strength, ductility, vertical strain for the achieved maximum load and vertical strain corresponding at 85% of the maximum load on the descending branch are presented. In the same table, the abbreviation CF is used for cleavage of concrete panel at its middle vertical axis, DB is used for the loss of bond between prefabricated-HSPRCC panel and concrete panel causing peeling of concrete surface followed by cleavage of concrete panel and CC is used for concrete crushing, TC is used for concrete crushing at the tip of the specimen and TE used for out of plane expansion of tip of the specimen. As seen in this table, the behaviour of all retrofitted specimens was improved in different extents, depending on the applied retrofitting schemes. Most of the specimens were

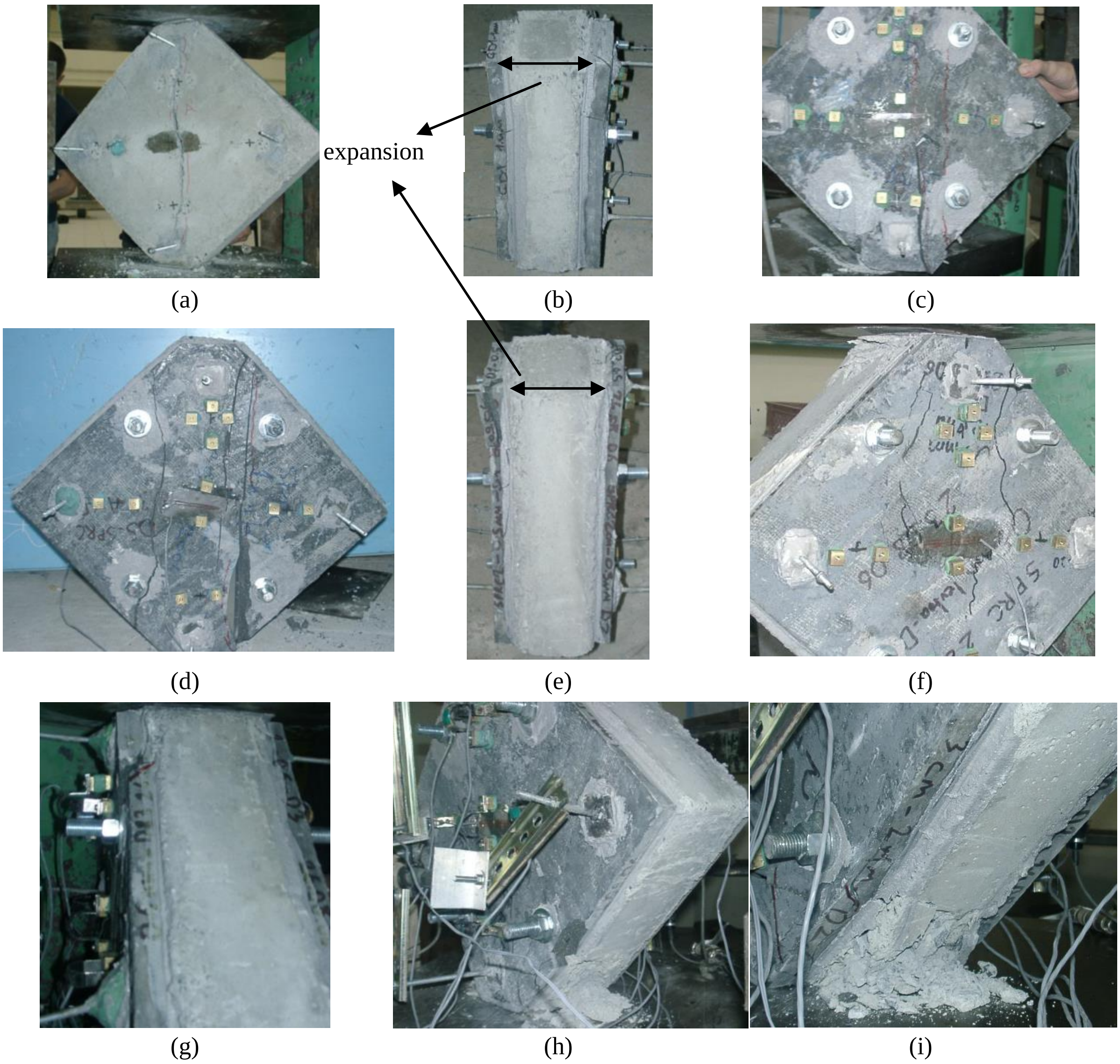


Fig. 15 Failure photos of the specimens, (a) Control, (b) DS-HSPRCC-30-1-CD1-A (c) DS-HSPRCC-30-2-CD1-A, (d) DS-HSPRCC-30-1-CD2-A, (e) DS-HSPRCC-20-0.5-D1-A, (f) DS-HSPRCC-20-0.5-D2-A, (g) DS-HPRCC-20-0.5-D3-A, (h) DS-HSPRCC-20-1-D2-A, (i) DS-HSPRCC-20-2-D2-A, (j) DS-HSPRCC-20-1-D2, (k) DS-HSPRCC-30-1-D2-A, (l) DS-HSPRCC-30-2-D2-A, (m) DS-HSPRCC-30-3-D2-A, (n) DS-HSPRCC-40-1-D2-A, (o) DS-HSPRCC-40-2-D2-A, (p) DS-HSPRCC-40-3-D2-A

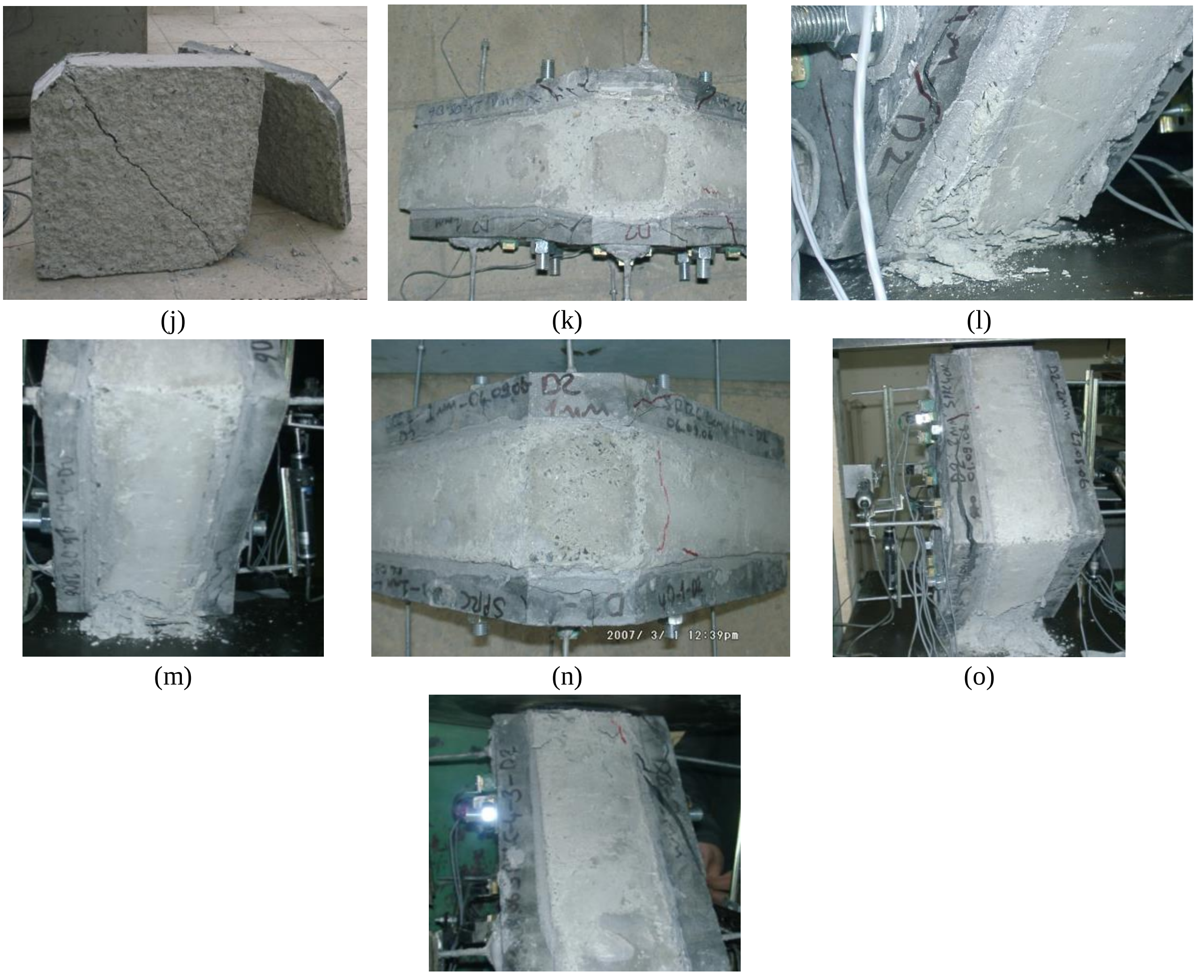

(j) (k) (l)

(m) (n) (o)

(p)

Fig. 15 Continued

failed finally due to concrete crushing and out of plane expansion of tip of the specimens. This clearly shows that failure mode change from brittle cleavage failure to more ductile failure tip expansion and crushing. Photos after failure of all specimens were given in Fig. 15. In original specimen sudden failure starts just after diagonal tension crack occur. As can be seen in Fig. 15 different then original specimen almost all retrofitted specimens failed because of tip expansion and crushing of concrete occur after diagonal tension crack.

Tests results were also described in terms of vertical load and vertical strain for evaluating global performances of specimens in terms of their load carrying and deformation capacities. As seen in Fig. 16, retrofitting, not only increased load carrying and displacement capacities, but also enhanced the toughness characteristics.

In addition to vertical load-vertical strain diagrams shear stress-shear strain relationships for all specimens are given in Fig. 17. It should be noted that the shear stress-shear strain relationships are given until the shear strain level, at which measuring devices worked perfectly. After these points, shear deformations continued to increase, while resisted load was decreasing. Shear stress-strain was calculated by using formulas given by ASTM E519 (2002), as given in Eqs. (1) and (2). In these equations, $\tau$, $P$, $b$ and $t$ are shear stress, vertical load, width and depth of the cross-section, respectively. $\gamma$ is the shear strain. $\Delta x_i$ and $\Delta y_i$ are the displacements in horizontal and vertical directions as shown in Figs. 1(a) and 14 (D-11, D-12, D-13, D-14). GL is the average gage length for displacement measurements. It should be noted that the gage lengths should be equal in each direction. Original specimens and specimen has no mechanical anchorage presented worse performance while specimen DS-HSPRCC-40-2-D2-A presented best performance as marked in Figs. 16 and 17.

$$\tau = 0.707P/(bt) \tag{1}$$

$$\gamma = (\Delta y_1 + \Delta y_2 + \Delta x_1 + \Delta x_2)/GL \tag{2}$$

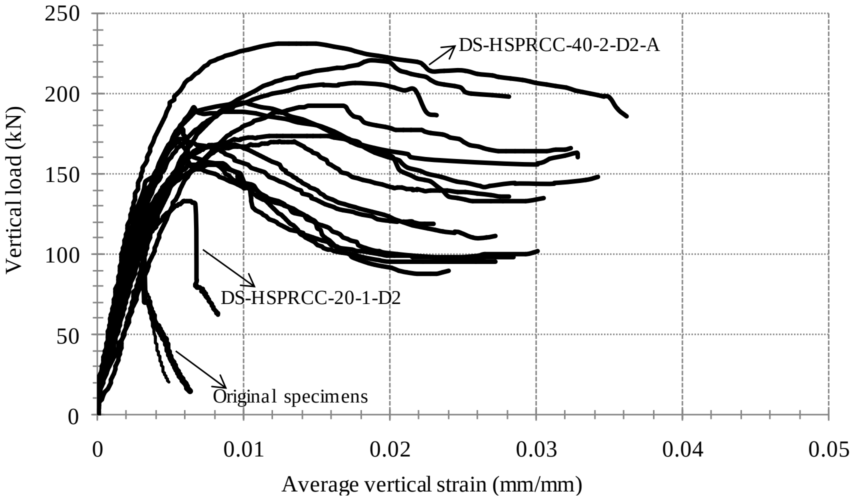


Fig. 16 Comparison of vertical load-average vertical strain relationships for all specimens

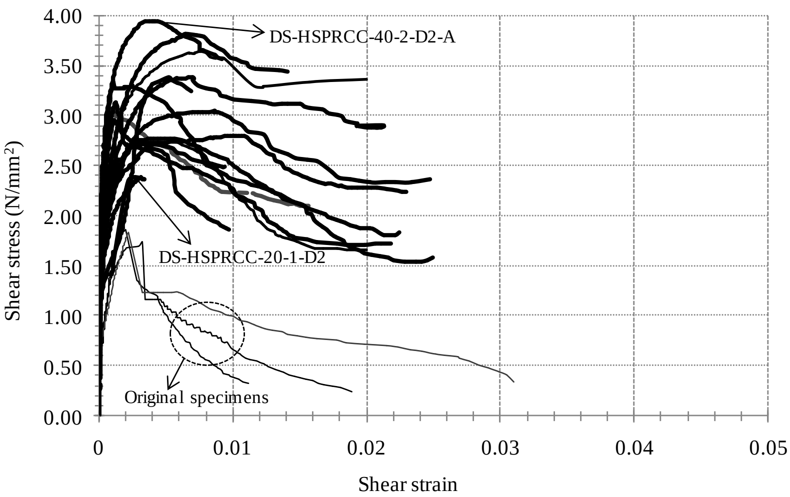


Fig. 17 Comparison of shear stress-shear strain relationships for all specimens

Table 4 Test results

| No | Specimens | Failure mode | Width of specimens (mm) | Maximum load (kN) | Shear strength (MPa) | Vertical strain at maximum load | Vertical strain at 85% of maximum vertical load on descending branch | Ductility | Increase in shear strength (%) |
|---|---|---|---|---|---|---|---|---|---|
| 1 | DS-O-a | CF | 106.00 | 104 | 1.73 | 0.0031 | 0.0032 | 1.03 | - |
| 2 | DS-O-b | CF | 106.80 | 112.5 | 1.86 | 0.0030 | 0.0031 | 1.03 | - |
| 3 | DS-O-c | CF | 103.25 | 107 | 1.83 | 0.00272 | 0.00278 | 1.02 | - |
| 4 | DS-HSPRCC-30-1-CD1-A | CF/TE/TC | 101.75 | 170 | 2.95 | 0.00558 | 0.01 | 1.8 | **57.7** |
| 5 | DS-HSPRCC-30-2-CD1-A | CF/TE/TC | 100.00 | 171 | 3.02 | 0.0055 | 0.0123 | 2.2 | **58.6** |
| 6 | DS-HSPRCC-30-1-CD2-A | CF/TE | 100.50 | 178 | 3.13 | 0.0057 | 0.0076 | 1.3 | **65.1** |
| 7 | DS-HSPRCC-20-0.5-D1-A | CF/TE/TC | 100.75 | 155 | 2.72 | 0.0075 | 0.0123 | 1.6 | **43.7** |
| 8 | DS-HSPRCC-20-0.5-D2-A | CF/TE/TC | 107.25 | 168 | 2.77 | 0.00796 | 0.0143 | 1.8 | **55.8** |
| 9 | DS-HSPRCC-20-0.5-D3-A | CF/TE/TC | 101.00 | 156 | 2.73 | 0.00708 | 0.0116 | 1.6 | **44.7** |
| 10 | DS-HSPRCC-20-1-D2-A | DB/TE/TC | 107.50 | 170 | 2.80 | 0.0123 | 0.0188 | 1.5 | **57.7** |
| 11 | DS-HSPRCC-20-2-D2-A | TE/TC | 100.75 | 173.5 | 3.04 | 0.0143 | 0.0215 | 1.5 | **60.9** |
| 12 | DS-HSPRCC-20-1-D2 | DB | 98.50 | 133 | 2.39 | 0.00587 | 0.0067 | 1.1 | **23.3** |
| 13 | DS-HSPRCC-30-1-D2-A | TE/TC | 101.50 | 194 | 3.38 | 0.00998 | 0.0195 | 2.0 | **79.9** |
| 14 | DS-HSPRCC-30-2-D2-A | TE/TC | 100.50 | 192.5 | 3.39 | 0.0159 | 0.028 | 1.8 | **78.5** |
| 15 | DS-HSPRCC-30-3-D2-A | TE/TC | 101.75 | 220 | 3.82 | 0.0187 | 0.028 | 1.5 | **104.0** |
| 16 | DS-HSPRCC-40-1-D2-A | CF/TE/TC | 101.00 | 191 | 3.34 | 0.0066 | 0.0192 | 2.9 | **77.1** |
| 17 | DS-HSPRCC-40-2-D2-A | CF/TE/TC | 103.50 | 231 | 3.94 | 0.0123 | 0.035 | 2.8 | **114.2** |
| 18 | DS-HSPRCC-40-3-D2-A | TE/TC | 100.00 | 206 | 3.64 | 0.0176 | 0.023 | 1.3 | **91.0** |

## 4. Evaluation of experimental results

Various parameters were investigated such as prefabricated-HSPRCC panel thickness, steel plate thickness, distribution of holes in steel plate, mechanical anchorage, application of steel plate at full surface or diagonal stripe.

As it can be seen in Table 4, the shear strengths increased between 23 and 114 for

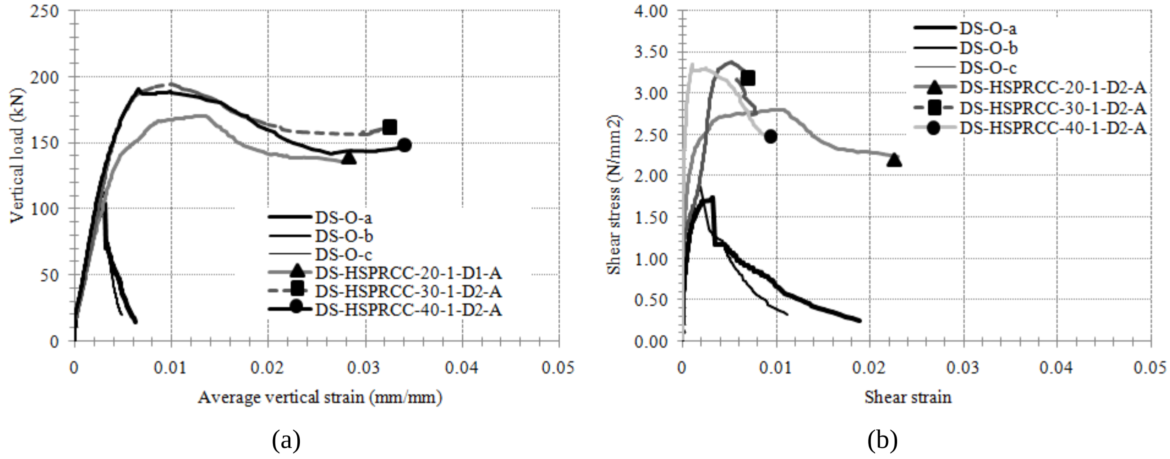


Fig. 18 Effect of HSPRCC thickness a) vertical load-average vertical strain, b) shear stress-shear strain relationship

prefabricated-HSPRCC panel retrofitted specimens. Enhancements in vertical strain correspond to the load level of 85% of the maximum load on descending branch of the load-vertical strain relationships are 121-1056% for prefabricated-HSPRCC panel retrofitted specimens.

Original specimen brittle failed due to formation of vertical tension crack. In the case of retrofitted specimens, the formation of vertical crack was retarded and growth of crack was decreased by prefabricated-HSPRCC panel. In specimen without additional anchorage system, worst behaviour in terms of deformability was observed.

Increase in shear strength and ductility in average excluding specimen DS-HSPRCC-20-1-D2 are 71% and 79%, respectively.

It is important to note that no considerable enhancement in strength would be possible by only increasing the thickness of the prefabricated-HSPRCC panel, unless appropriate anchoring of the panel is made to the concrete specimen.

### 4.1 Effect of prefabricated-HSPRCC panel thickness

Only difference between retrofitted specimens given in Fig. 18 is the thickness of prefabricated-HSPRCC panel. Load capacity increases with thickness of prefabricated-HSPRCC panels however load capacities are the same for 30 and 40-mm thicknesses. On the other hand as can be seen in Fig. 18(b) stiffness of the retrofitted specimens tends to increase with prefabricated-HSPRCC panel thicknesses. Stiffness of all specimens is nearly the same in the view of vertical load-average vertical strain diagrams, Fig. 18(a).

### 4.2 Effect of steel plate thickness

In order to investigate effect of steel plate thicknesses on the behaviour of retrofitted specimens having 30 mm and 40 mm HSPRCC panel thicknesses were compared. Improvement with increasing steel plate thicknesses can be seen from all diagrams given in Fig. 19. However improvement in behaviour is more compulsive in case of 40-mm HSPRCC panel thicknesses.

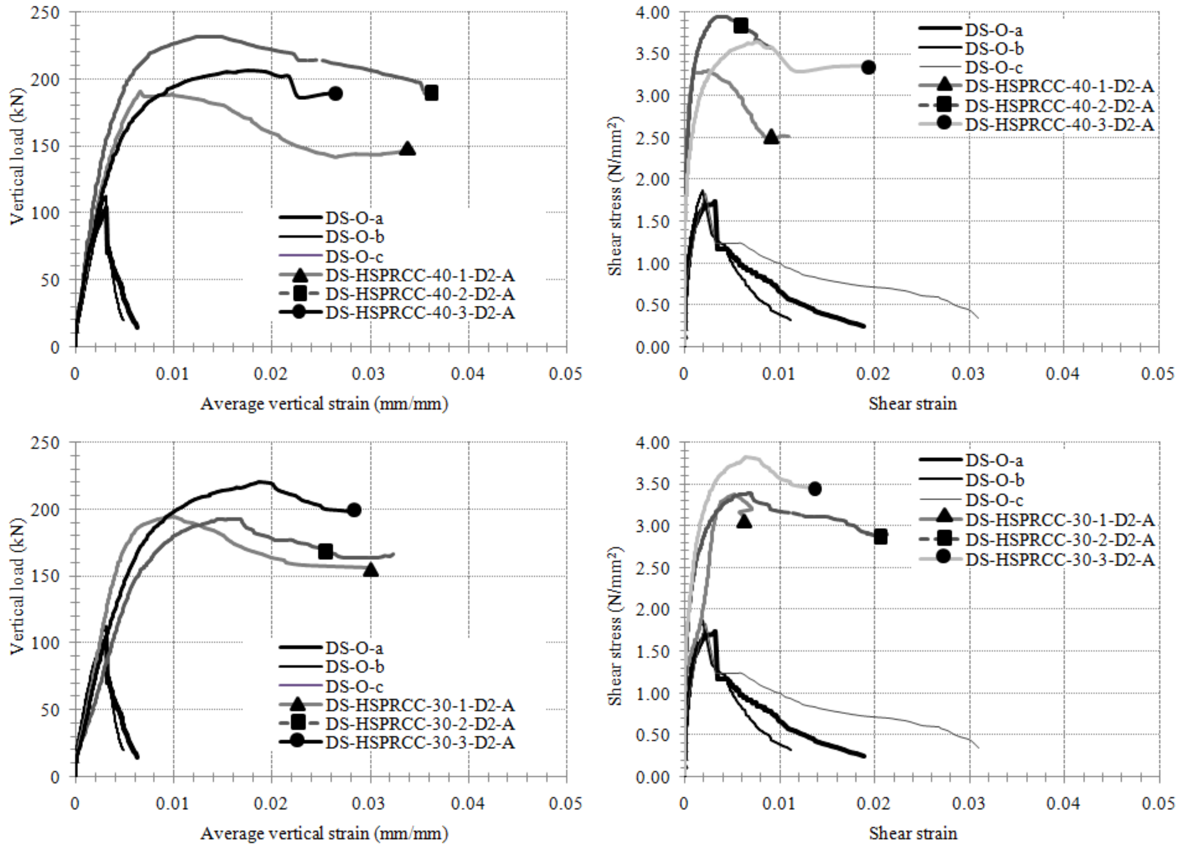


(a) (b)

Fig. 19 Effect of steel plate thickness a) vertical load-average vertical strain, b) shear stress-shear strain relationship

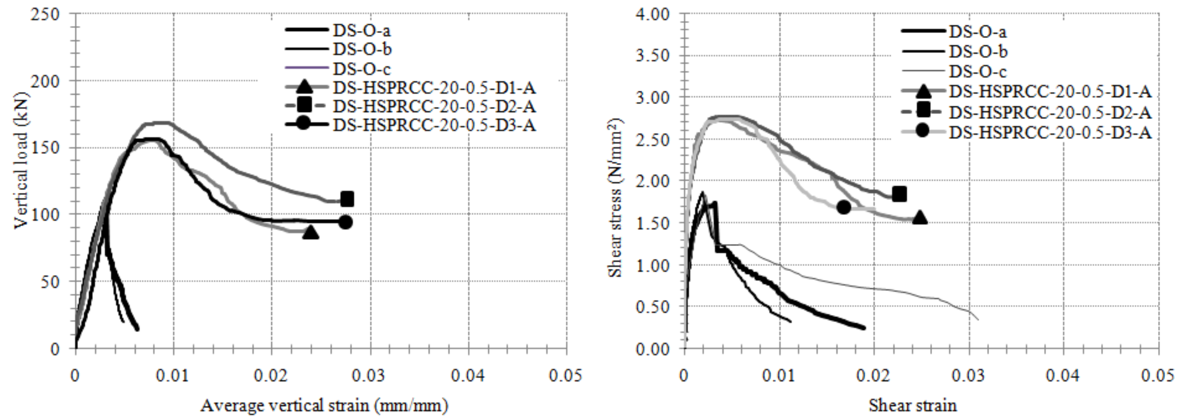


(a) (b)

Fig. 20 Effect of hole distribution a) vertical load-average vertical strain, b) shear stress-shear strain relationship

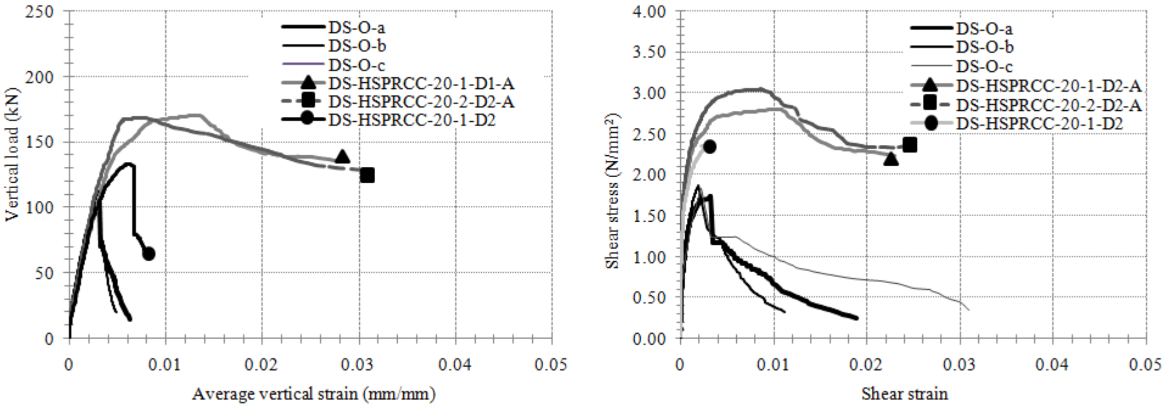


(a) (b)

Fig. 21 Effect of mechanical anchorage (a) vertical load-average vertical strain, (b) shear stress-shear strain relationship

### *4.3 Effect of hole distribution*

Effect of hole distribution was investigated in case of 20-mm prefabricated-HSPRCC panel thickness and 0.5-mm steel plate thickness. Puncture orientation D2 seem to be more effective than the others, Fig. 20.

### *4.4 Effect of mechanical anchorage*

Effect of mechanical anchorage can clearly be seen by comparing specimens DS-HSPRCC-20-1-D2-A and DS-HSPRCC-20-1-D2 where only difference is mechanical anchorage between these two specimens. As seen in Fig. 21 mechanical anchorage improved both load capacity and displacement capacity of the specimens substantially.

## 5. Mechanical evaluation

Behaviour of the original and retrofitted specimens was studied by using simple mechanic rules. As mentioned before there are different failure mechanisms listed in Table 4. For clearly understanding failure mechanism and predicting vertical load capacities, possible failure mechanisms were investigated separately. All possible failure mechanisms and corresponding vertical load capacities are listed in Table 5. Furthermore contribution of prefabricated-HSPRCC panel to the vertical load capacities of retrofitted specimens was given separately as well.

According to simple mechanic shear stress of the specimen under point diagonal load as illustrated in Fig. 22 is given in Eq. (1). A similar equation is also given by ASTM E519 (2002). $P_{\max.}$ is the maximum diagonal load applied vertically, b and t are the edge dimension and width of square member, respectively. Eq. (1) can be re-written as Eq. (2) considering $\tau$ is equal to concrete tension strength $f_t$. Concrete direct ($f_{ct}$) and splitting ($f_t$) tensile strengths are considered as $f_{ct} = 0.35\sqrt{f_c^{'}}$ and $f_t = 0.5\sqrt{f_c^{'}}$, respectively as defined in Requirements for Design and

Table 5 Evaluation of test results

| No | Specimens | Maximum load-Experimental (kN) | Maximum load prediction corresponding to possible failure mechanisms (kN); Cleavage failure of concrete | Slip of prefabricated-HSPRCC panel | Cleavage failure of high strength concrete | Crushing of concrete around the hole | $P_{teoretical}$=Cleavage failure of concrete panel + HSPRCC panel (kN) | $P_{exp.}/P_{theoretical}$ |
|---|---|---|---|---|---|---|---|---|
| 1 | DS-O-a | 104 | 84.8 | - | - | - | - | 1.23 |
| 2 | DS-O-b | 112.5 | 85.4 | - | - | - | - | 1.32 |
| 3 | DS-O-c | 107 | 82.6 | - | - | - | - | 1.30 |
| 4 | DS-HSPRCC-30-1-CD1-A | 170 | 78.3 | 156 | 200.6 | 138 | 278.8 | 0.61 |
| 5 | DS-HSPRCC-30-2-CD1-A | 171 | 76.9 | 156 | 200.6 | 277 | 277.5 | 0.62 |
| 6 | DS-HSPRCC-30-1-CD2-A | 178 | 77.3 | 156 | 200.6 | 231 | 277.9 | 0.64 |
| 7 | DS-HSPRCC-20-0.5-D1-A | 155 | 77.5 | 156 | 133.7 | 191 | 211.2 | 0.73 |
| 8 | DS-HSPRCC-20-0.5-D2-A | 168 | 82.5 | 156 | 133.7 | 202 | 216.2 | 0.78 |
| 9 | DS-HSPRCC-20-0.5-D3-A | 156 | 77.7 | 156 | 133.7 | 302 | 211.4 | 0.74 |
| 10 | DS-HSPRCC-20-1-D2-A | 170 | 82.7 | 156 | 133.7 | 403 | 216.4 | 0.79 |
| 11 | DS-HSPRCC-20-2-D2-A | 173.5 | 77.5 | 156 | 133.7 | 806 | 211.2 | 0.82 |
| 12 | DS-HSPRCC-20-1-D2 | 133 | 75.8 | 156 | 133.7 | 403 | 155.8 | 0.85 |
| 13 | DS-HSPRCC-30-1-D2-A | 194 | 78.1 | 156 | 200.6 | 403 | 278.7 | 0.70 |
| 14 | DS-HSPRCC-30-2-D2-A | 192.5 | 77.3 | 156 | 200.6 | 806 | 277.9 | 0.69 |
| 15 | DS-HSPRCC-30-3-D2-A | 220 | 78.3 | 156 | 200.6 | 1209 | 278.8 | 0.79 |
| 16 | DS-HSPRCC-40-1-D2-A | 191 | 77.7 | 156 | 267.4 | 403 | 345.1 | 0.55 |
| 17 | DS-HSPRCC-40-2-D2-A | 231 | 79.6 | 156 | 267.4 | 806 | 347.0 | 0.67 |
| 18 | DS-HSPRCC-40-3-D2-A | 206 | 76.9 | 156 | 267.4 | 1209 | 344.4 | 0.60 |
| | | | Average | | | | | 0.80 |

Construction of Reinforced Concrete Structures (TS 500 2000). In case of simple shear loading and for elastic isotropic material shear stresses can be assumed to be equal to principal stresses. If we arrange Eq. (1) by using tensile strength of the concrete ($f_t$) and then the failure load ($P_{max.}$) of the panel can be estimated with Eq. (2).

$$\tau = \frac{P_{max.}\sqrt{2}}{2bt} \quad \text{(MPa)} \tag{1}$$

$$P_{max.} = \frac{2 f_t bt}{\sqrt{2}} \quad \text{(N)} \tag{2}$$

Retrofitted specimen without mechanical anchorage failed as a result of loss of bond between prefabricated-HSPRCC panel and specimen causing peeling of concrete surface followed by cleavage of specimen. Considering this type of failure vertical load capacity can be obtained. Failure of specimen happens as soon as after cracking of concrete panel through debonding of prefabricated-HSPRCC panel showed that debonding of prefabricated-HSPRCC panel limit the capacity of retrofitted specimen. Contact area providing bonding between prefabricated-HSPRCC panel and specimen was shown in Fig. 23. So, lateral force provided by bonding can be calculated with Eq. (3)

$$F = A_T \times f_{ct} = A_T \times 0.35\sqrt{f_c^{'}} \tag{3}$$

Bonding shear stress can be taken as concrete direct tensile strength. Shear stress can be calculated from lateral $F$ force with Eq. (4).

$$\tau = \frac{F}{h_p t} \tag{4}$$

Finally vertical load capacity corresponding to the slip of prefabricated-HSPRCC panel was obtained by combining Eqs. (2)-(4), Eq. (5).

$$P_{max.} = \frac{2\tau bt}{\sqrt{2}} = \frac{2(F / h_p t)bt}{\sqrt{2}} = \frac{0.7 A_T b\sqrt{f_c^{'}}}{\sqrt{2} h_p} \tag{5}$$

Above formulation could be used for retrofitted specimen with mechanical anchorage easily by obtaining lateral force $F$ illustrated in Fig. 23. Direct tensile strength of HSPRCC high-strength mortar obtains from cylinder splitting strength (8.8 MPa). Splitting tensile strength multiplied by 0.7 (0.35/0.50) to obtain direct tensile strength as defined in TS 500 (2000).

Lateral load capacities of retrofitted specimens with mechanical anchorage were obtained by summing up vertical load capacities corresponding to cleavage failure of concrete panel and prefabricated-HSPRCC panel. However as observed from tests of retrofitted specimen including anchorage application specimen finally failed due to concrete expansion and crushing of tip of the specimen. So, vertical load capacities expected to be smaller than predicted vertical load capacities. With considering effect of specimen tip concrete crushing in the mechanical evaluation more reasonable prediction can be made. Under increasing compression stress tip of the specimens tend to expansion to out of plane direction and force prefabricated-HSPRCC panel bend to out of plane. So, confinement provided by prefabricated-HSPRCC plate is related to bending stiffness of prefabricated-HSPRCC panel. Bending stiffness of prefabricated-HSPRCC panel increases with mainly due to prefabricated-HSPRCC panel thickness increase.

After cracking of prefabricated-HSPRCC panel, perforated steel is not only influenced by direct tension force, but there is also bending. Perforated steel plate is effective especially after cracking of prefabricated-HSPRCC panel and it especially increases ductility substantially.

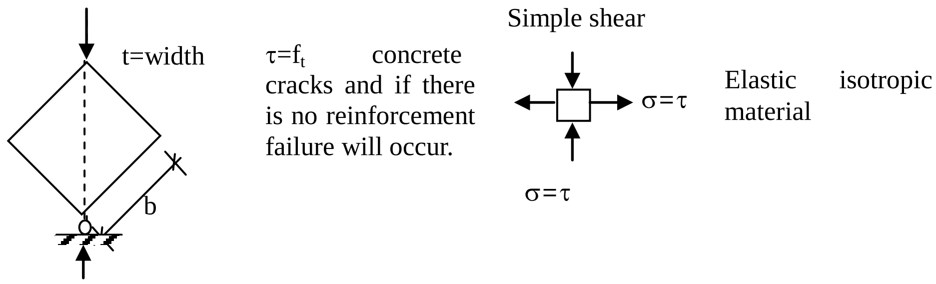


Fig. 22 Panel under vertical load

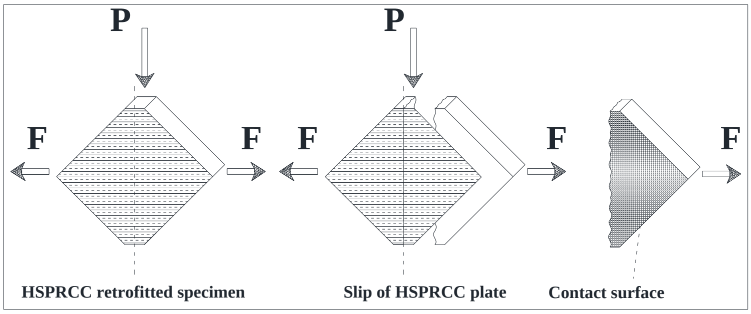


Fig. 23 Debonding of HSPRCC plate from concrete member under vertical load

There is another possible failure mode which was not mentioned in Table 4 because it did not observed during the test is that concrete may crush due to stress concentration around holes of perforated steel plate, Fig. 24. These holes are very effective to provide bond between HSPRCC high-strength mortar and steel plate. Anchorage of steel plate to high-strength concrete of prefabricated-HSPRCC panel is provided by two main mechanisms. 1- bonding between steel plate surface to high-strength concrete, 2- mechanical interlocking between holes and high-strength concrete. If we assume that all the lateral load would only be transferred thorough compression force around holes we can calculate a conservative virtual vertical load limits causing crushing of concrete around the holes, Fig. 24. This limit would give us a reasonable prediction on this type of failure. The same approach summarized with Eq. (1) and (4) can be used to calculate vertical load capacity corresponding compression failure of high-strength concrete around the holes. An only difference here is the lateral *F* load. Eq. (6) was used to calculate total lateral load F for crushing of concrete at all holes easily.

$$F=(2*H_N)*(D_p/2)*t_s*\sigma_{HSPRCC} \tag{6}$$

In this equation $H_N$ is the total number of holes, $D_p$ is the perimeter of the hole, $t_s$ thicknesses of the steel plate and $\sigma_{HSPRCC}$ is compression strength of the HSPRCC high-strength mortar. Crushing of concrete around hole limit for all three type of hole distribution in case of three different steel plate thicknesses shown in Table 6. Parameters related to properties of holes are also given in this table. These limiting loads are also given in Table 5 in order to compare with other vertical load limits. Table 5 and Table 6 clearly show that none of the specimen failed due to concrete crushing around edges of holes.

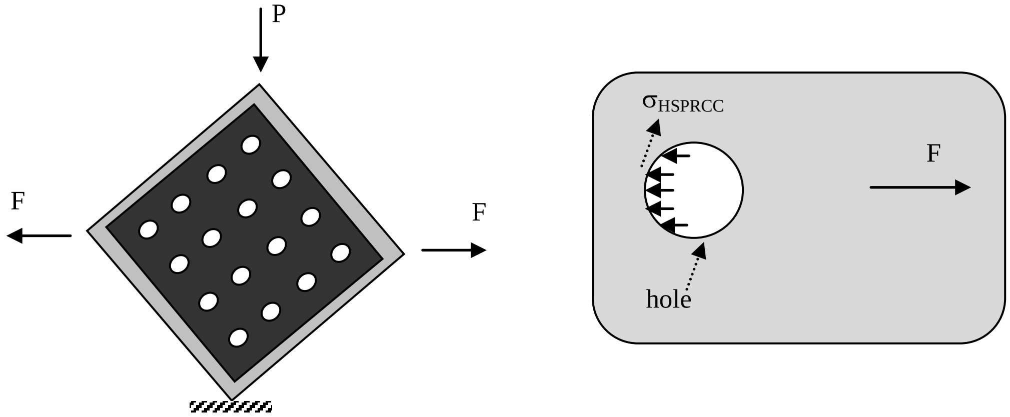


Fig. 24 Lateral *F* load induced from vertical load developed high compression stress around the holes

Table 6 Load capacity corresponding HSPRCC plate concrete crushing around edge of holes

| Hole type | $H_N$ | $H_D$ (mm) | $H_P$ (mm) | Steel Plate area (mm$^2$) | Total hole area (mm$^2$) | $\rho_H$ (%) | $t_s$=0.5 mm | | | $t_s$=1 mm | $t_s$=2 mm | $t_s$=3 mm | $P_{exp.}$ (kN) |
|---|---|---|---|---|---|---|---|---|---|---|---|---|---|
| | | | | | | | $F$-kN | $\tau$-MPa | $P$-kN | $P$-kN | $P$-kN | $P$-kN | |
| D1 | 24-4 | 15-24 | 47.1-75.4 | 127919 | 6051 | 4.7 | 83.1 | 1.7 | 96 | 191 | 383 | 574 | 155 |
| D2 | 32 | 30 | 94.2 | 127919 | 22620 | 17.7 | 174.9 | 3.6 | 202 | 403 | 806 | 1209 | 168-170-174-133-194-193-220-191-231-206 |
| D3 | 32 | 45 | 141.4 | 127919 | 50894 | 39.8 | 262.4 | 5.3 | 302 | 605 | 1209 | 1814 | 156 |
| CD1 | 22 | 15 | 47.1 | 42525 | 3888 | 9.1 | 60.1 | 1.2 | 69 | 139 | 277 | 416 | 170-171 |
| CD2 | 22 | 25 | 78.5 | 42525 | 10799 | 25.4 | 100.2 | 2.0 | 115 | 231 | 462 | 693 | 178 |

Note: $H_N$: Number of holes, $H_D$: Diameter of holes, $H_P$: Perimeter of holes, $\rho_H$ (%):ratio of holes area to total steel area, $t_s$: thickness of steel plate, $F$: Lateral force exerted on specimen, $P$: Vertical load, $P$-Exp.: Experimentally measured vertical load capacity.

## 6. Conclusions

In this study, a new retrofitting technique through utilization of prefabricated-HSPRCC panels that can be used for shear retrofitting of columns, beams, shear walls and beam-column joints was developed. Low-strength concrete diagonal panels were tested under diagonal tension before and after retrofitting with prefabricated-HSPRCC panels by utilizing a simple testing method for experimental analysis. According to test results, considerably higher shear strength and deformability were possible through this retrofitting application. Prefabricated-HSPRCC panels sustained tensile forces exerted in diagonal direction and they limited shear deformation. Sudden brittle type of failure were turned to a more energy dissipated a ductile failure type. To predict experimental behaviour of reference and prefabricated-HSPRCC retrofitted specimens, simple mechanic rules were being carried out. Theoretical results were in agreement with experimental data in terms of strengths in some extend.

It should also be noted that the proposed retrofitting technique is a promising and a more practical alternative to the current retrofitting methods. The application of the proposed method is easier, quick and economically feasible. Furthermore since the prefabricated-HSPRCC panels are fabricated before application the disturbance to the occupants would be the minimum. In addition prefabricated-HSPRCC panel composes high tensile strength and ductility properties of steel with high compression strength and good durability properties of high performance concrete. Nevertheless, it is important to mention that the current study is a primary study carried out on small scaled specimens and further research on full scale tests is necessary to obtain more generally applicable results.

## Acknowledgments

The experimental study is financially supported by Tasdildiren and Iston ready mix concrete company. The contributions of Orkun Incecik during experimental work are also acknowledged. Thanks are due to Prof. A. Ilki of Istanbul Technical University for his valuable contributions. ITU material and structural engineering laboratories acknowledged for providing their facilities to carry out the experimental work

## References

Abdulhameed, S., Wu, E. and Ji, B. (2013), “Mechanical prestressing system for strengthening reinforced concrete members with prestressed carbon-fiber-reinforced polymer sheets”, *J. Perform. Constr. Facil*., **29**(3), 04014081.

Alcocer, S.M. and Jirsa, J.O. (1993), “Strength of reinforced concrete frame connections rehabilitated by jacketing”, *ACI Struct. J*., **90**(3), 249-261.

Amoury, T. and Ghobarah, A. (2002), “Seismic rehabilitation of beam column joints using GFRP sheets.” *Eng. Struct.*, **24**, 1397-1407.

Antonopoulos, C.P. and Triantafillou, T.C. (2003), “Experimental investigation of FRP-strengthened RC beam-column joints”, *ASCE J. of Compos. Constr*., **7**(1), 39-49.

ASTM E519 (2002), “Standard test method for diagonal tension (shear) in masonry assemblages”, *American Society for Testing Materials*, USA.

Barros, J.A.O., Costa, I.G. and Ventura-Gouveia, A. (2011), “CFRP flexural and shear strengthening technique for RC beams: experimental and numerical research”, *J. Adv. Struct. Eng.*, **14**(3), 551-557.

Bedirhanoglu, I. (2009), “The behavior of reinforced concrete members with low strength concrete under earthquake loads: an investigation and improvement”, PhD Thesis, Istanbul Technical University, Istanbul, Turkey, DOI: 10.13140/2.1.1286.8480

Bedirhanoglu, I., Ilki, A., Incecik, O. and Kumbaar, N. (2008), “Retrofit of concrete panels with prefabricated hpfrcc plates”, *14 WCEE, The 14th World Conference on Earthquake Engineering*, Beijing,

China.
Bedirhanoglu, I., Ilki, A., Pujol, S. and Kumbasar, N. (2010), "Seismic behavior of joints built with plain bars and low-strength concrete", *ACI Struct. J.*, **107**(3), 300-310.
Bedirhanoglu, I., Ilki, A. and Kumbasar, N. (2013), "Precast fiber reinforced cementitious composites for seismic retrofit of deficient rc joints-A pilot study", *Eng. Struct.*, **52**, 192-206.
Bedirhanoglu, I. (2014), "A practical neuro-fuzzy model for estimating modulus of elasticity of concrete", *Struct. Eng. Mech.*, **51**(2), 249-265.
Biddah, A.M.S., Ghobarah, A. and Aziz, T.S. (1997), "Upgrading of non ductile reinforced concrete frame connections", *ASCE J. Struct. Eng.*, **123**(8), 1001-1010.
Collins, M.P., Vecchio, F.J. and Mehlhorn, G. (1985), "An international competition to predict the response of reinforced concrete panels", *Can. J. Civil Eng.*, **12**, 624-644.
Durham, SA., Heymsfield, E. and Jones, J.X. (2009), "Retrofitting of precat bridge beams with carbon fiber-reinforced polymer strips for shear capacity", *ASCE J. Perform. Constr. Facil.*, **23**(4), 219-226.
Gabor, A., Bennani, A., Jacquelin, E. and Lebon, F. (2006), "Modelling approaches of the in-plane shear behaviour of unreinforced and FRP strengthened masonry panels", *Compos. Struct.*, **74**(3), 277-288.
Gergely, J., Pantalides, C.P. and Reaveley, L.D. (2000), "Shear strengthening of RC T-joints using CFRP composites", *ASCE J. Compos. Constr.*, **4**(2), 56-64.
Ghobarah, A. and Said, A. (2001), "Seismic rehabilitation of beam-column joints using FRP laminates", *J. Earthq. Eng.*, **5**(1), 113-129.
Garcia, R., Hajirasouliha, I. and Pilakoutas, K. (2010), "Seismic Behaviour of Deficient RC Frames Strengthened with CFRP Composites", *Eng. Struct.*, **32**(10), 3075-3085.
Hamad, B.S. and Ibrahim, F.G. (2009), "Effect of FRP confinement on bond strength of hooked bars: normal strength concrete structures", *ASCE J. Compos. Constr.*, **13**(4), 279-291.
Ilki, A., Bedirhanoglu, I., Candan, Y. and Kumbaar, N. (2007), "Retrofit of low strength concrete panels with frp sheets", FRPRCS-8 University of Patras, Patras, Greece.
Ilki, A., Bedirhanoglu, I. and Kumbasar, N. (2008), "Seismic retrofit of beam-column joints with FRP sheets", *Proc., 5th International Conference on Advanced Composite Materials in Bridges and Structures (ACMBS-V)*, September, Winnipeg, Manitoba, Canada.
Ilki, A., Peker, O., Karamuk, E., Demir, C. and Kumbasar, N. (2008), "FRP retrofit of low and medium strength circular and rectangular reinforced concrete columns", *J. Mater. Civil Eng.*, **20**(2), 169-188.
Ilki, A., Demir, C., Bedirhanoglu, I. and Kumbasar, N. (2009), "Seismic retrofit of brittle and low strength RC columns using fiber reinforced polymer and cementitious composites", *J. Adv. Struct. Eng.*, **12**(3), 325-347.
Ilki, A., Bedirhanoglu, I. and Kumbasar, N. (2011), "Behavior of FRP retrofitted joints built with plain bars and low-strength concrete", *ASCE J Compos. Constr.*, **15**(3), 312-326.
Itoh, M., Katoh, Y. and Kanakubo, F.T. (2000), "Influence of concrete type and strength to shear behavior of RC panel", *Tran. JPN Concrete Inst.*, **22**, 393-398.
Kanakubo, T. and Shindo, M. (1997), "Shear behavior of fiber-mesh reinforced plates." *Proceedings of the Third International Symposium*, *Non-Metallic (FRP) Reinforcement for Concrete Structures*, **2**, 317-324.
Karayannis, C.G., Chalioris, C.E. and Sirkelis, G.M. (2008), "Local retrofit of exterior RC beam-column joints using thin RC jackets-An experimental study", *Earthq. Eng. Struct. Dyn.*, **37**, 727-746.
Karbhari, V. and Gao, Y. (1997), "Composite jacketed concrete under uniaxial compression-verification of simple design equations", *J. Mater. Civil Eng.*, **9**(4), 185-193.
Lee, K.S., Lee, S.H. and Shin, S.W. (2013), "Shear behavior of reinforced concrete beams strengthened by epoxy mortar panel with steel fibers", *J. Adv. Struct. Eng.*, **16**(6), 987-1000.
Li, V.C., Stang, H. and Krenchel, H. (1993), "Micromechanics of crack bridging in fiber-reinforced concrete", *Mater. Struct.*, **26**(162), 486-494.
Lin, M.L., Chen, P.C., Tsai, K.C., Yu, Y.J. and Liu, J.G. (2010), "Seismic steel jacketing of rectangular RC bridge columns for the mitigation of lap-splice failures", *Earthq. Struct. Dyn.*, **39**(15), 1687-1710.
Lu, X. and Hsu, C.T.T. (2006), "Behavior of high strength concrete with and without steel fiber reinforcement in triaxial compression", *Cement Concrete Res.*, **36**(9), 1679-1685.

Mosallam, A.S. (2000), "Strength and ductility of RC frame connections strengthened with quasi-isotropic laminates", *Compos. Part B*, **31**(6-7), 481-497.

Mosalam, K.M., Stephen, A.M. and Rojansky, M. (2003), "Evaluation of seismic performance and retrofit of lightweight reinforced concrete shear walls", *ACI Struct. J.*, **100**(6), 693-703.

Mukherjee, A. and Joshi, M. (2005), "FRPC reinforced concrete beam-column joints under cyclic excitation", *Compos. Struct.*, **70**(2), 185-199.

Nagaprasad, P., Sahoo, D.R. and Rai, D.C. (2009), "Seismic strengthening of RC column using external steel cage", *Earthq. Struct. Dyn.*, **38**(14), 1563-1586.

Niroomandi, A., Maheri, A., Maheri, M.R. and Mahini, S.S. (2010), "Seismic performance of ordinary RC frames retrofitted at joints by FRP sheets", *Eng. Struct.*, **32**(8), 2326-2336.

Pantelides, C.P., Okahashi, Y. and Reaveley, L.D. (2008), "Seismic rehabilitation of reinforced concrete frame interior beam-column joints with FRP composites", *ASCE J. Compos. Constr.*, **12**(4), 435-445.

Prota, A., Nanni, A., Manfredi, G. and Cosenza, E. (2003), "Capacity assessment of RC subassemblages upgraded with CFRP", *J. Reinf. Plast. Compos.*, **22**(14), 1287-1304.

Shah, S.P. (1991), "Do fibers increase the tensile strength of cement-based matrices", *ACI Mater. J.*, **88**(6), 595-602.

Shannag, M.J., Barakat, S. and Jaber, F. (2001), "Structural repair of shear-deficient reinforced concrete beams using SIFCON", *Mag. Concrete Res.*, **53**(6), 391-403.

Shannag, M.J., Abu-Dyya, N. and Abu-Farsakh, G. (2005), "Lateral load response of high performance fiber reinforced concrete beam-column joints", *Constr. Build. Mater.*, **19**(7), 500-508.

TS138 EN 10002-1 (2004), "Metallic materials-tensile testing-Part 1: method of test at ambient temperature", Turkish Standards Institute (TSE), Ankara, Turkey.

TS 500 (2000), "Requirements for design and construction of reinforced concrete structures", Turkish Standards Institute (TSE), Ankara, Turkey.

Tsonos, A.G. (2002), "Seismic repair of exterior R/C beam-to-column joints using two sided jackets", *Struct. Eng. Mech.*, **13**(1), 17-34.

Tsonos, A.G. (2008), "Effectiveness of CFRP-jackets in post-earthquake and pre-earthquake retrofitting of beam-column subassemblages", *Eng. Struct.*, **30**, 777-793.

Tsonos, A.G. (2010), "Performance enhancement of R/C building columns and beam-column joints through shotcrete jacketing", *Eng. Struct.*, **32**(3), 726-740.

Xiao, Y. and Wu, H. (2000), "Compressive behavior of concrete confined by carbon fiber composite jackets", *J. Mater. Civil Eng.*, **12**(2), 139-146.

Xiao, Y. (2004), "Applications of FRP composites in concrete columns", *J. Adv. Struct. Eng.*, **7**(4), 335-343.

Valluzzi, M.R., Tinazzi, C. and Modena, C. (2002), "Shear behavior of masonry panels strengthened by frp laminates", *Constr. Build. Mater.*, **16**(7), 409-416.

Vecchio, F.J. and Nieto, M. (1991), "Shear-friction tests on reinforced concrete panels", *ACI Struct. J.*, **88**(3), 371-379.

Wu, H., Sun, P. and Teng, J. (2010), "Development of fiber-reinforced cement-based composite sheets for structural retrofit", *J. Mater. Civil Eng.*, **22**(6), 572–579.

Yen, J.Y.R. and Chien, H.K. (2010), "Steel plates rehabilitated RC beam-column joints subjected to vertical cyclic loads", *Constr. Build. Mater.*, **24**(3), 332-339.

Yoshitake, I., Inamori, A., Hamada, S. and Hisabe, N. (2006), "Pure shearing behaviour of concrete element with carbon fiber sheet", *Proceedings of the 2nd International Congress*, Naples, Italy.

*CC*

## Notation

*The following symbols are used in this paper:*

| | | |
|---|---|---|
| $A_T$ | = | total contact area between prefabricated-HSPRCC and concrete panel |
| $b$ | = | width of the cross-section |
| $F$ | = | lateral force |
| $f_{ct}$ | = | direct tensile strength |
| $f_t$ | = | splitting tensile strength |
| $GL$ | = | average gage length |
| $H_D$ | = | diameter of holes |
| $H_N$ | = | total number of holes |
| $H_p$ | = | perimeter of holes |
| $h_p$ | = | height of the concrete panel |
| $P$ | = | vertical load |
| $P_{exp.}$ | = | experimental vertical load capacity |
| $P_{\max.}$ | = | maximum vertical load |
| $t$ | = | depth of the concrete panel's cross-section |
| $t_s$ | = | steel plate thickness |
| $\sigma_{HSPRCC}$ | = | compression strength of HSPRCC |
| $\rho_H$ (%) | = | ratio of holes area to total steel area |
| $\tau$ | = | shear stress |
| $\gamma$ | = | shear strain |
| $\Delta x_i$ | = | horizontal displacement |
| $\Delta y_i$ | = | vertical displacement |